arXiv:astro-ph/0004153v1 11 Apr 2000

Optimal Masks for Low-Degree Solar Acoustic Modes

T. Toutain
Département CASSINI, Observatoire de la Côte d'Azur, Nice, France

A. G. Kosovichev
W.W.Hansen Experimental Physics Laboratory,
Stanford University, Stanford, CA 94305-4085

ABSTRACT

We suggest a solution to an important problem of observational helioseismology of the separation of lines of solar acoustic (p) modes of low angular degree in oscillation power spectra by constructing optimal masks for Doppler images of the Sun. Accurate measurements of oscillation frequencies of low-degree modes are essential for the determination of the structure and rotation of the solar core. However, these measurements for a particular mode are often affected by leakage of other p modes arising when the Doppler images are projected on to spherical-harmonics masks. The leakage results in overlaping peaks corresponding to different oscillation modes in the power spectra. In this paper we present a method for calculating optimal masks for a given (target) mode by minimizing the signals of other modes appearing in its vicinity. We apply this method to time series of 2 years obtained from Michelson Doppler Imager (MDI) instrument on board SOHO space mission and demonstrate its ability to reduce efficiently the mode leakage.

Subject headings: Sun:oscillations

1. Introduction

Accurate measurements of frequencies and other physical properties of solar oscillations are crucial for understanding the internal structure and dynamics of the Sun. Up to now the determination of low-degree p-mode parameters like cyclic frequency ν, linewidth or frequency splitting is based on fitting the so-called m-ν diagrams obtained by projecting time series of solar images (usually Dopplergrams) on to a basis of spherical harmonics of angular degree l and azimuthal order m. Because only one hemisphere of the Sun is observed the projection on to spherical harmonics is not orthogonal. This results in leakage of modes which makes the line fitting quite complicated especially when modes overlap with the target mode. We have therefore decided to apply a method originally developed by Kosovichev (1986) based on a singular value decomposition (SVD) technique in order to minimize the leakage.

We discuss in Sec. 2 the principle of the method, and introduce the concepts of 'global' and 'local' optimal masks. The global optimal masks are designed to minimize the contribution of all modes except the target one. The local masks minimize only modes within a narrow frequency interval centered at the target mode. In Sec. 3 we show the theoretical efficiency of the method compared to the usual spherical harmonics projection. In Sec. 4 we illustrate this method with a 2-year time series of MDI LOI-proxy data, obtained by rebinning of the original 1024 by 1024 CCD pixels into 180 bins (Hoeksema et al., 1998; Scherrer et al., 1995) according to the shape of the LOI instrument (Appourchaux et al. 1997).

2. The optimal-mask method

The aim of the optimal masks (Gough, 1984 and Christensen-Dalsgaard, 1984) is to find an optimal linear combination of N signals arising from N bins of the solar image in order to produce a time series containing mainly the contribution of a mode with given l and m, the so-called target mode, and minimizing the contribution of others modes. It is particularly important to minimize the contribution of modes which are close to the target mode in the power spectrum. These are mainly modes of the same rotationally split multiplet as the target mode. At frequencies about 2.5 mHz and higher the linewidth of p modes becomes larger than the separation between the peaks. Therefore, it is important to separate the overlapping modal lines. We describe this method in the application to the MDI LOI-proxy data. However, this method is quite general and can be applied to other spatially resolved helioseismic data.

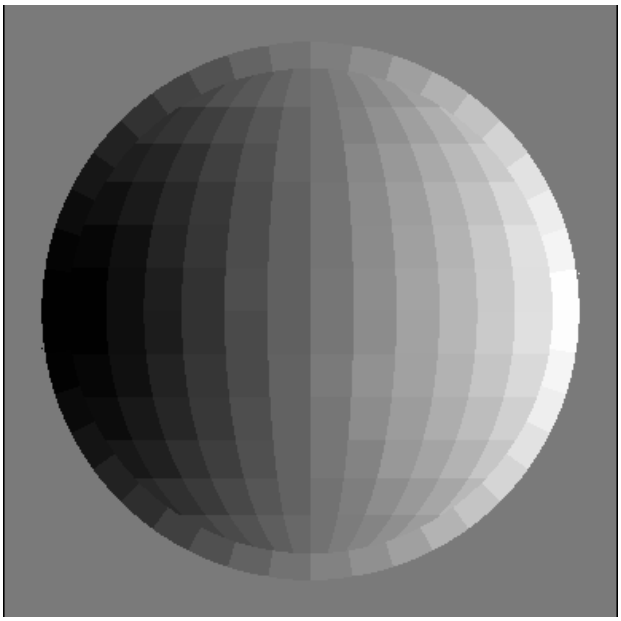

Fig. 1.— An example of MDI LOI-proxy Dopplergrams. The full-disk 1024x1024-pixel MDI Dopplergrams are rebinned on board SOHO into 180 bins with the boundaries along heliospheric meridians and parallels. The variation from dark to light colors is due to solar rotation.

Because we observe only one hemisphere of the Sun, the commonly used spherical-harmonic masks are not able to remove all the components of the target mode multiplet. Instead of using the spherical harmonics masks we apply a SVD method to derive the optimal masks. To apply this method we first need to model the signal produced in each image bin by a mode of given angular degree l, azimuthal order m and radial order n. For simplicity, in this paper, the horizontal component of velocity is neglected because we are only interested in low-degree p modes. The inclusion of the horizontal component is straightforward, and generally improves the quality of the optimal masks in the low-frequency part of the solar oscillation spectrum where this component becomes significant. Hence, to the first order, the signal of a normal mode in each pixel j of the CCD detector is:

$$v_{nlm}^{(j)}(t) = \Re\left\{V_{nlm} e^{i\omega_{nlm}t} s_{lm}^{(j)}(t)\right\}, \qquad (1)$$

where V_{nlm} is the mode amplitude, ω_{nlm} is the mode frequency, and $s_{lm}^{(j)}(t) = Y_{lm}[\theta_j^*(t), \phi_j^*(t)]\mu_j$ is the sensitivity function which depends on the spatial eigenfunction, spherical harmonic Y_{lm}, and the factor μ_j arising from the projection of the radial velocity onto the line of sight. Both Y_{lm} and μ_j are expressed in terms of the heliographic coordinates, $\theta_j^*(t)$ and $\phi_j^*(t)$, of the pixels, which are generally functions of time t. We have to take into account the fact that the orientation of the solar image, which is usually described by two angles of the rotation axes with respect to the ecliptics, P_0 and B_0, and the image size on the detector are possibly changing with time. The time dependences of the P_0 and B_0 angles should therefore be taken into account by rotating the spherical coordinates accordingly. In our case the variations of the image size were not taken into account because the data were combined into fixed 180 bins on board spacecraft prior to any mask application. An example of the rebinned Dopplergrams ('MDI LOI-proxy') is shown in Fig. 1.

The kth signal of each of the N bins is obtained by averaging the signals coming from N_k CCD pixels withing this bin as defined by the mapping between the MDI pixels and the LOI-proxy bins:

$$v_{nlm}^{(k)}(t) = \Re\left\{V_{nlm}e^{i\omega_{nlm}t}S_{lm}^{(k)}(t)\right\}, \qquad (2)$$

where $S_{lm}^{(k)}(t) = \frac{1}{N_k}\sum_{j=1}^{N_k} s_{lm}^{(j)}(t)$ is $S_{lm}^{(k)}$ is the sensitivity of bin k to a normal mode of angular degree l and order m. To extract the signal of a target mode of n_0, l_0 and m_0 we combine the N signals with N weights $w_{n_0l_0m_0}^{(1)}$,...,$w_{n_0l_0m_0}^{(N)}$:

$$v_{n_0l_0m_0}(t) = \sum_{k=1}^{N} w_{n_0l_0m_0}^{(k)} v_{nlm}^{(k)}(t) =$$
$$\Re\left\{V_{nlm}e^{i\omega_{nlm}t}\left[\sum_{k=1}^{N} w_{n_0l_0m_0}^{(k)} S_{lm}^{(k)}(t)\right]\right\}. \qquad (3)$$

Ideally, if the sum in the square brackets is equal to the product of two Kroneker symbols, $\delta_{ll_0}\delta_{mm_0}$, then $v_{n_0l_0m_0}(t)$ consists only of the signal of the target mode. However, in practice, this sum does not represent $\delta_{ll_0}\delta_{mm_0}$ and contains not only the target mode but also contributions from other modes.

Vector $\mathbf{w}_{n_0l_0m_0} \equiv \{w_{n_0l_0m_0}^{(1)}, ..., w_{n_0l_0m_0}^{(N)}\}$ defines an optimal mask if this vector is chosen to maximize the signal for the target mode and minimizes the signals for other, say M, modes located close to the target mode in the Fourier domain. These conditions can be written as a minimization of the quadratic form:

$$r = ||\mathbf{S}\cdot\mathbf{w} - \mathbf{I}||^2, \qquad (4)$$

where $\mathbf{S}$ is a $(M+1)\times N$ matrix with elements $S_{nlm}^{(k)}(t)$ and $\mathbf{I}$ is a $(M+1)$-element vector with elements $\delta_{ll_0}\delta_{mm_0}$, l_0 and m_0 being the angular degree and order of the target mode.

Finding $\mathbf{w}$ is equivalent to finding a least-squares solution to the system of linear equations, $\mathbf{S}\cdot\mathbf{w} = \mathbf{I}$. Depending on M, the number of modes we want to minimize, we have a system which is over-determined (N > M+1) or under-determined (N < M+1). For both cases the problem is efficiently solved using the singular value decomposition (SVD) of the matrix $\mathbf{S}$ (e.g. Press et al. 1992). This method optimally solves the linear system and its solution $\mathbf{w}$ gives the optimal mask. This mask provides an efficient filtering of the selected M modes. Of course, the minimization is less efficient when M is large. There is therefore a trade-off between the number of modes to minimize and the efficiency of this minimization.

Matrix $\mathbf{S}$ describes the sensitivity of each detector bin to the mode of oscillation. For the special case of an under-determined system (N < M+1) this technique is equivalent to the technique of diagonalization of the leakage matrix (Appourchaux et al., 1998). The SVD method allows us to consider general cases. With this technique we can specifically decide which modes must be filtered and to what extend their contribution to the power spectra should be reduced, making the technique extremely flexible. In practice we filter as much as possible the modes having frequencies falling in a given frequency window around the target making a kind of local cleaning of the spectra. We therefore call the corresponding masks 'local optimal masks' to distinguish from the 'global optimal masks' obtained when minimizing the contribution of all the modes not only those around the target mode. The larger the window around the target the more modes have to be minimized, and thus the less efficient is the filtering. In principle we are able to remove efficiently as many modes as the number of the binned signals, 180 in our case. Above that number the SVD acts as a least square minimization and the modes cannot be fully filtered. In practice, the efficiency of the filtering depends on the selected mode set and the noise level.

The solar noise obviously will be less filtered than modes by the masks because its spatial structure is

incoherent. Thus the signal-to-noise ratio of the target mode depends on the mask. More efficient masks typically require higher weights $w_{nlm}^{(k)}$, and, therefore amplify the noise. This leads to the trade-off between the mask efficiency and the noise level. To adjust this trade-off we slightly modify Eq. (4) and add the noise contribution through a regularization term. Then the quadratic form to minimize is

$$r = ||\mathbf{S} \cdot \mathbf{w} - \mathbf{I}||^2 + \alpha ||\mathbf{n} \cdot \mathbf{w}||^2, \qquad (5)$$

where $\mathbf{n} = \{n^{(1)}, ..., n^{(N)}\}$ is the vector of the standard deviation of the noise in each of the N bins, and α is the regularization parameter. The SVD technique is still applicable here. Eq. (4) corresponds to the case of α=0 which means no regularization.

The noise level is estimated by taking the standard deviation of the signal in each bin, assuming the main contributor is the solar noise. Generally, the noise level is the lowest at the center of the solar disk and increases toward the limb. Table 1 gives a sample of the relative noise level of the MDI measurements as a function of the angular distance from the disk center. Obviously, the absolute noise level is not required for Eq.(5).

The regularization parameter α is chosen such as the amplitudes of the filtered modes is reduced to the level of noise. It turns out that the signal-to-noise ratio obtained with the local optimal masks is similar to what is obtained with spherical-harmonic masks, though it may be somewhat smaller (up to 50%). Only for l=0 the difference in the signal-to-noise ratio between the two masks can reach a factor of two or more. Because of solar noise we also avoid using the limb bins. These bins improve very little the efficiency of the masks but contribute significantly to the noise. Removing not only limb bins but also the next round of bins helps to increase the signal-to-noise ratio at low frequencies for $l = 0$ modes, but this is not effective for modes of higher degrees.

The power of this technique is also that the optimal masks for any P_0 and B_0 angles are easily obtained applying the spherical harmonic rotation matrix to the optimal masks with P_0=0 and B_0=0. Therefore it is possible as for MDI to apply the optimal masks for each day according to the value of B_0 which is changing with time without recomputing the SVD problem which is a heavy computational task .

Table 1: Relative noise level, n, in the MDI data as a function of the angular distance, d, from the disk center.

d, deg.	1.72	11.0	20.5	30.7	42.1	56.1
n	1.00	1.15	1.40	1.73	1.99	2.27

3. Comparison of spherical-harmonic masks and optimal masks

In order to test the efficiency of the optimal masks we compute how these masks filter the modes versus the target mode and compare to the spherical-harmonic masks. We assume that each mode leads to a velocity signal which is a perfect spherical harmonic projected onto the line of sight. The degree range of modes is given by the properties of the detector. The 180-bin detector (the LOI-proxy) shown in Fig. 1 is sensitive up to modes l=15. The higher-degree modes do not contribute significantly to the observed signal. Therefore, in the global masks we restrict the mode range from $l = 0$ to 15.

The results of the global and local masks are represented in the form of a map (called hereafter amplitude map) showing the relative amplitude of the modes identified with the doublet (l, m) for l between 0 and 6 and m between $-l$ and $+l$.

Figure 2 shows, as an example for a target l=1 and m=1, the way various masks filter the unwanted modes. On top left we used the disk-integrated signal which leads to the usual problem of mode blending between m=$\pm$ 1. It is well-known (Chang, 1997) that this blending especially bias the determination of frequency splitting. For the spherical-harmonic masks (top right), the blending is smaller but still there is the same problem. Using the local optimal masks for a frequency window of $\pm$15 μHz we are able to reduce below the noise level the m=-1 as well as the l=3,6 and 9 modes which were also interfering with the target mode. Note that global masks (bottom, right) as expected do not remove perfectly these modes because the number of modes to filter (around 3000) exceeds the number of bins by a large factor. We give another example for a l=4, m=3 mode in Fig. 2. Applying the local optimal masks should therefore lead to clean power spectra around the target mode as shown in next section using the MDI data.

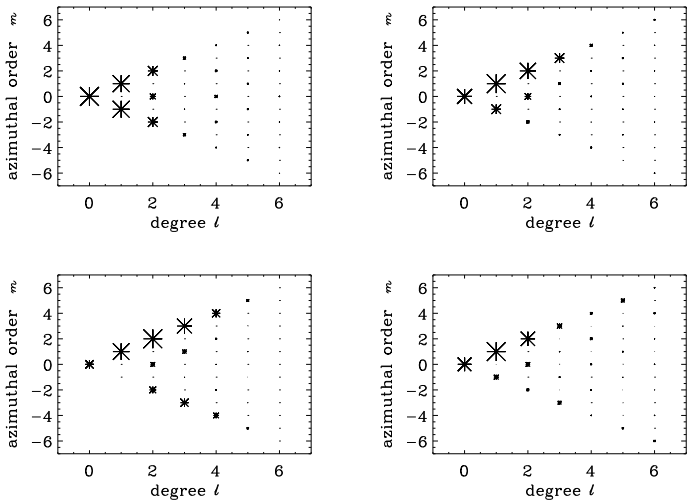

Fig. 2.— Amplitude maps for a disk-integrated mask (top, left), spherical-harmonics masks(top, right),local optimal masks (bottom, left) and global optimal masks (bottom right) with target l=1, m=1. The size of the symbols on this map is proportional to mode amplitudes.

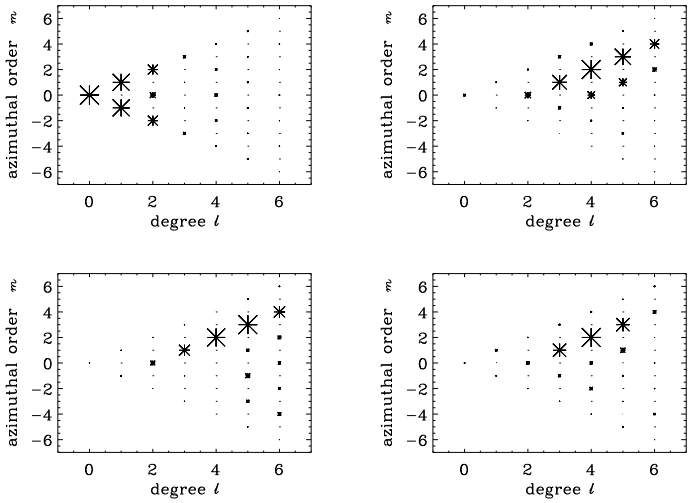

Fig. 3.— The same as in Fig. 2 but for l=4, m=2.

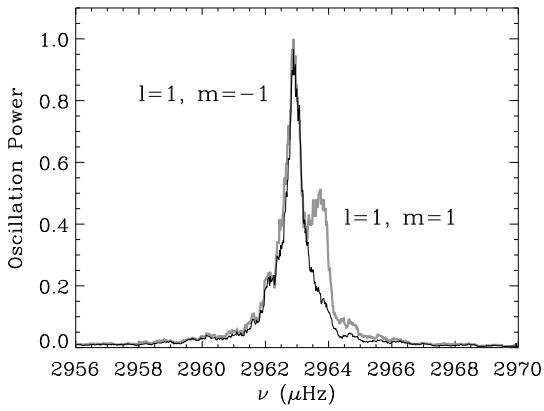

Fig. 4.— Power spectrum for l=1 m=-1 mode using the spherical-harmonic mask (grey curve) and local optimal masks (black curve).

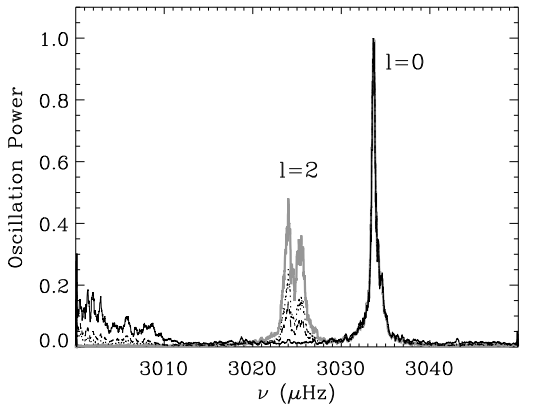

Fig. 5.— Power spectrum around target mode l=0 at 3034 μHz for local optimal masks with a different regularization parameter α: zero (black solid curve), small (dotted curve), large (dashed curve) and for integrated velocity (grey curve).

4. Optimal masks applied to MDI data

In order to apply the optimal masks to MDI data we need in principle to take account of the time-dependence of the signal due to the displacement of the image on the detector and change of its size as the SOHO-Sun distance is changing. However, for the low-degree modes this effect is expected to be small, and was neglected in these studies.

The larger effect would result from the variations of the images orientation angles P_0 and B_0. However, in the MDI observations the P_0 is quite stable and much less than 1 degree. The B_0 varies between -7 and + 7 degrees during a year. However, we found that these variations lead only to non-significant variations of our optimal masks. Therefore, we adopt the mean value, B_0=0.

As an example, Figure 4 shows overlapped two pieces of power spectra of a l=1, $m = -1$ mode, one obtained with the standard spherical harmonic masks (grey curve) and the other one with the local optimal masks (black curve). In the first case, the power spectrum shows a significant leakage of the l=1 m=1 mode which belongs to the same rotationally split multiplet. This mode partially overlaps with the target mode. In the optimal mask spectrum, the contribution of this mode is reduced to the level of noise. As previously noticed the signal-to-noise ratio is better with the spherical-harmonic masks but the leakage mode is strongly blended with the target one leading to bias in the estimation of mode parameters. Modes of l=6 and 9 were also filtered for this case. The singular value cut-off was chosen to be of the order of the numerical accuracy and no regularization was applied which means optial filtering with a slightly larger noise level.

Figure 5 shows the effect of regularization for a target mode of l=0, where the modes of l=2, 5, 8, 11 and 15 are filtered out in a window of $\pm 15\mu$Hz around the target mode. For α=0 the contiguous l=2 mode multiplet at 3024 μHz is reduced to noise level whereas as α increases this mode becomes larger and the noise level decreases. We found that in most cases the optimal masks with $\alpha = 0$ work sufficiently well.

5. Conclusions

Mode leakage which results in overlapping mode peaks in solar oscillation power spectra is one of the most significant problems in observational helioseismology. It may lead to significant errors in the determination of mode frequencies and other properties. We have shown that this problem can be efficiently solved by using the optimal masks which are applied to series of solar images and reduce the signals of solar modes in a narrow frequency interval around a target mode to the level of noise. The optimal mask, however, may increase the noise level. Therefore, the filtering efficiency of the masks has to be balanced with the noise level. This is achieved by a regularization technique. We have demonstrated in the case of low-degree modes that the optimal mask technique allows us efficiently isolate individual modes in rotationally split multiplets, which are unresolved in the commonly used disk-integrated data, and also isolate modes in the case of overlapped multiplets of different angular degree. The optimal masks are quite efficient for filtering out unwanted modes as long as their number is less or of the order of the number of solar image bins. We used the MDI LOI-proxy data to calculate the optimal masks. However, this method is quite general and can be used for any spatially resolved helioseismic data.

The method has been applied for the determination of the central low-degree frequencies by Toutain et al (1999). In a future paper, we will present the results for rotational splitting of low-degree modes.

REFERENCES

Appourchaux, T, Andersen, B., Fröhlich, C., Jimenez, A., Telljohann, Udo, Wehrli, C., 1997, Sol. Phys. 170, 27.

Appourchaux, T. and Gizon, L., Rabello-Soares, M.-C., 1998, A&AS 132, 107

Chang, H.-Y., 1997, PhD thesis, University of Cambridge.

Christensen-Dalsgaard, J. 1984, in Solar Seismology From Space, ed. R.K. Ulrich, J. Harvey, E.J. Rhodes, and J. Toomre, Pasadena: Jet Propulsion Laboratory, 219.

Gough, D.O., and Latour, J. 1984, Astron. Express, 1, 9.

Hoeksema, J.T., Bush, R.I., Mathur, D., Morrison, M., and Scherrer, P.H., 1998, in: Sounding Solar and Stellar Interiors, Symp. IAU 181, eds. J. Provost, F.-X. Schmider, Poster Vol., Univ. Nice, p.31.

Kosovichev, A.G. 1986, Bull. Crimean Astrophys. Obs., 75, 19.

Press, W.H., Teukolsky, S.A., Vetterling, W.T., and Flannery, B.P. Numerical Recipes, Second Edition, Cambridge University Press, 1992.

Scherrer,P.H., Bogart, R.S., Bush, R.I., Hoeksema, J.T., Kosovichev, A.G., Schou, J., Rosenberg, W., Springer, L., Tarbell, T.D., Title, A., Wolfson, C.J., Zayer, I. and the MDI engineering team, 1995, Sol. Phys. 162, 129.

Toutain, T., Appourchaux, T., Fröhlich, C., Kosovichev, A. G., Nigam, R., and Scherrer, P. H., 1999, ApJ, 506, L147.

This 2-column preprint was prepared with the AAS LaTeX macros v4.0.